Localization of Wave Propagation in Disordered Periodic Structures

G. Q. Cai* and Y. K. Lin†
Florida Atlantic University, Boca Raton, Florida

A structure designed to be spatially periodic in its configuration cannot be exactly periodic due to material, geometric, and manufacturing variabilities. Such variabilities are random, and their presence (often referred to as disorder) can reduce the ability of the structure to transmit waves from one location to another. The phenomenon is known as vibration confinement or localization. A new perturbation scheme is developed in this paper on the basis of probability theory to calculate the average exponential decay rate of wave transmission with respect to the distance of transmission, called the localization factor. Account is also taken of structural damping. The new scheme permits successive improvement of accuracy, making it applicable to either weak, strong, or moderate localization. Moreover, the analysis is based on a generic periodic structure; thus, it is not restricted to a specific set of governing equations. These are achieved by taking into account reflections from nearby disordered cell-units successively and substituting the ensemble average for the sequential average of certain statistical properties of the cell units on the basis of spatial ergodicity. Application of the method is illustrated by an example, and the results are compared with Monte Carlo simulations.

Introduction

MANY engineering structures are designed to be composed of identically constructed cell units that are connected end to end to form a spatially periodic array. Such structures are known as periodic structures and have been the subject of extensive investigations for more than 30 years (e.g., Refs. 1–6). One well-known property common to periodic structures is their alternate wave-passage and wave-stoppage frequency bands. If a periodic structure is undamped and is infinitely long, then disturbances at frequencies within the wave-passage bands can propagate indefinitely, whereas those within the wave-stoppage bands diminish in a short distance.

However, due to material, geometric, and manufacturing variabilities, a structure designed to be periodic can never be exactly periodic. The departure from ideal periodicity is known as disorder, which must be taken into account in a realistic analysis. To our knowledge, the earliest work dealing with disordered engineering periodic structures from a probabilistic point of view was that of Soong and Bogdanoff using a perturbation approach. They studied the variability of the natural frequencies and normal modes for free vibration,[7] as well as the frequency response and impulse response for forced vibration of a finite chain of mass-spring-damper units due to the variability of the unit properties.[8] Subsequently, Lin and Yang[9,10] applied a similar approach to a beam on many supports, with the span lengths between neighboring supports and the bending rigidities of various spans differing randomly from the respective nominal design values.

The ability to transmit disturbances indefinitely within the wave-passage bands is reduced when the ideal periodicity in a periodic structure is disrupted. This is known as the localization effect, first predicted by Anderson[11] in a celebrated paper concerning the transport of electrons in an atomic lattice, which is essentially a disordered three-dimensional periodic system. Anderson's work has found important applications in solid-state physics. Since then, numerous papers on localization have appeared in the physics literature.[12]

Obviously, localization also occurs in disordered periodic structural systems, but its theoretical investigation is more difficult than that of a one-dimensional atomic lattice since governing equations for structural systems are generally more complex. Using the models of a chain of coupled pendula and a vibrating string constrained by attached masses and springs, Hodges[13] provided an excellent explanation for the confinement of vibration and for localized normal modes as a result of structural irregularity. Subsequently, he and Woodhouse[14] calculated the so-called localization factor for one of the systems, characterizing the average exponential decay of vibration amplitude with respect to the distance from the disturbance. Two perturbation schemes were devised to treat the cases of weak and strong localizations, depending on the relative measures of disorder and internal (namely, unit-to-unit) coupling.

Pierre[15] also calculated the localization factor for both weak and strong localization, using both the wave propagation and normal mode formulations and obtained essentially same results. He devised two perturbation schemes to treat the two cases when the ratio of the disorder measure to the internal coupling measure is either large or small. As expected, his results were not very accurate when this ratio is of order one.

The first analysis of a generic disordered periodic system was given by Kissel,[16] who used the concept of wave transmission and reflection, and a limit theorem on the product of random matrices due to Furstenberg.[17] For a wave motion propagating at a wave-passage frequency, no reflection would occur at the unit-to-unit interface if the system were exactly periodic. When two adjoining units are not identical, total transmission is no longer possible, and some reflection will take place at the interface. However, Kissel's analysis requires that the reflection be small; thus, his results are valid only for the case of weak localization.

Unlike previous investigators, Kissel has also explored the case of multicoupling, namely, the internal coupling that permits the transmission of several types of waves. An outline was provided of an approach based on the multiplicative ergodic theorem of Oseledets.[18] Unfortunately, the theorem only predicts the existence of a localization factor (analogous to the Liapunov exponent in the time domain, of interest to

Received Sept. 28, 1989; revision received Feb. 19, 1990.

*Research Assistant, Center for Applied Stochastics Research.
†Schmidt Chair and Director, Center for Applied Stochastics Research. Associate Fellow AIAA.

Oseledets), without providing the necessary clues regarding how it can be calculated.

The ability to treat a generic system is clearly very desirable, since the analysis is applicable to a general class of problems, not restricted to a specific type of governing equations. Furthermore, it appears easier to extend such an analysis to the case of multicoupling, which is likely to occur in many practical structural systems. Thus, it is also the objective of the present paper to calculate the localization factor for a generic disordered periodic structure. A new perturbation scheme is developed here that permits successive improvement of the accuracy, making it applicable to either weak, moderate, or strong localization. The additional accuracy is obtained by taking into account reflections from additional nearby cells. Account is also taken of structural damping; thus, the results are more useful to practicing engineers. The key to the successful development of a simple theory under rather general settings is the substitution of ensemble averages for sequential averages of certain statistical properties of the structure on the basis of spatial ergodicity. The simplicity of the new method is illustrated by applying it to a multiply-supported Euler-Bernoulli beam with an additional torsional spring at each support. The accuracy of the results is substantiated by Monte Carlo simulations. Only monocoupling at the unit-to-unit interfaces is considered in detail. The case of multicoupling will be discussed further in another paper.

Wave Transmission and Reflection Matrices

Consider two typical cell units in a disordered periodic structure, denoted as cells n and $n+1$ and shown in Fig. 1a. The relation between the state vector at the left end of cell unit n and that at the left end of cell unit $n+1$ may be written as follows:

$$\begin{Bmatrix} w(n-1_l) \\ f(n+1_l) \end{Bmatrix} = [T(n)] \begin{Bmatrix} w(n_l) \\ f(n_l) \end{Bmatrix} \tag{1}$$

where each w is a p-dimensional vector of generalized displacements, each f is a p-dimensional vector of generalized forces, and $[T(n)]$ is a $2p \times 2p$ transfer matrix associated with the nth cell. It is implied in Eq. (1) that the motion is timewise sinusoidal, and the displacements and forces are interpreted as their complex-valued amplitudes. Because of disorder, $[T(n)]$ is generally different from the ideal transfer matrix $[T]$ associated with the ideal design condition of exact periodicity. Nevertheless, it is always possible to write

$$[T(n)] = [P(n)][T] \tag{2}$$

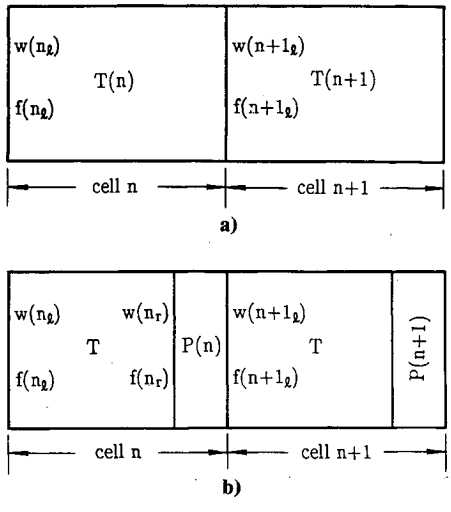

Fig. 1 State vector representation: a) original system; b) equivalent system.

which means that the effect of disorder in the nth cell can be lumped at its right end and represented by a "point" transfer matrix $[P(n)]$. In other words, the original system shown in Fig. 1a can be replaced by an equivalent system shown in Fig. 1b. In typical transfer matrix analysis[19] a point transfer matrix is used to relate state vectors on the two sides of a structural discontinuity that may arise from a concentrated mass, spring, damper, etc. However $[P(n)]$ in Eq. (2) is merely a mathematical device, and it may even correspond to, e.g., a negative mass.

Refer to Fig. 1b and write

$$\begin{Bmatrix} w(n_r) \\ f(n_r) \end{Bmatrix} = [T] \begin{Bmatrix} w(n_l) \\ f(n_l) \end{Bmatrix} \tag{3a}$$

$$\begin{Bmatrix} w(n+1_l) \\ f(n+1_l) \end{Bmatrix} = [P(n)] \begin{Bmatrix} w(n_r) \\ f(n_r) \end{Bmatrix} \tag{3b}$$

Each state vector in Eq. (3a) can be transformed into a wave vector using

$$\begin{Bmatrix} w(n_l) \\ f(n_l) \end{Bmatrix} = [D] \begin{Bmatrix} \mu^r(n_l) \\ \mu^l(n_l) \end{Bmatrix} \tag{4a}$$

$$\begin{Bmatrix} w(n_r) \\ f(n_r) \end{Bmatrix} = [D] \begin{Bmatrix} \mu^r(n_r) \\ \mu^l(n_r) \end{Bmatrix} \tag{4b}$$

where the columns in the transformation matrix $[D]$ are the eigenvectors of $[T]$. These eigenvectors must be arranged in a particular order, which will become apparent in the subsequent development. We then obtain a wave-transfer relationship,

$$\begin{Bmatrix} \mu^r(n_r) \\ \mu^l(n_r) \end{Bmatrix} = [D]^{-1}[T][D] \begin{Bmatrix} \mu^r(n_l) \\ \mu^l(n_l) \end{Bmatrix} = \begin{bmatrix} \lambda_1 & & & 0 \\ & \lambda_2 & & \\ & & \ddots & \\ 0 & & & \lambda_{2p} \end{bmatrix} \begin{Bmatrix} \mu^r(n_l) \\ \mu^l(n_l) \end{Bmatrix} \tag{5}$$

in which λ_j, $j = 1, ..., 2p$ are the eigenvalues of the ideal transfer matrix $[T]$. Each λ_j represents the ratio of complex-valued amplitudes of one type of wave at the two ends of an ideal cell unit. Since damping generally exists in a physical structure, the magnitude of a wave decreases when it propagates across a cell. Thus, each eigenvalue accounts for the reduction of the wave magnitude, as well as the change of phase from one side of an ideal cell unit to another. It is known that eigenvalues of a transfer matrix are reciprocal pairs.[3] For every λ_j there exists another $\lambda_k = \lambda_j^{-1}$. If $|\lambda_j| < 1$, then $|\lambda_k| = |\lambda_j|^{-1} > 1$. They correspond to two identical types of waves, except that one is right-going and the other is left-going. The limiting case $|\lambda_j| = 1$ can only occur in an undamped structure and only at a frequency in one of the wave-passage frequency bands.

We arrange the order of eigenvectors in $[D]$ so that the corresponding eigenvalues are in ascending order; thus, $|\lambda_j| < 1$ if $j = 1, 2, ..., p$, and $|\lambda_j| > 1$ if $j = p+1, p+2, ..., 2p$. Equation (5) may then be rewritten as follows:

$$\begin{Bmatrix} \mu^r(n_r) \\ \mu^l(n_r) \end{Bmatrix} = \begin{bmatrix} \Lambda & 0 \\ 0 & \Lambda^{-1} \end{bmatrix} \begin{Bmatrix} \mu^r(n_l) \\ \mu^l(n_l) \end{Bmatrix} \tag{6}$$

where

$$\Lambda = \begin{bmatrix} \lambda_1 & & 0 \\ & \ddots & \\ 0 & & \lambda_p \end{bmatrix} \tag{7}$$

Or, alternatively,

$$\begin{Bmatrix} \mu^l(n_l) \\ \mu^r(n_r) \end{Bmatrix} = [S] \begin{Bmatrix} \mu^r(n_l) \\ \mu^l(n_r) \end{Bmatrix} \tag{8}$$

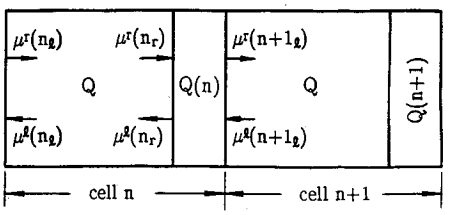

Fig. 2 Wave vector representation, equivalent system.

with

$$[S] = \begin{bmatrix} 0 & \Lambda \\ \Lambda & 0 \end{bmatrix} \tag{9}$$

The meanings of the superscripts r and l associated with the wave vectors μ are now clear; they indicate the right-going and the left-going wave groups, respectively, transmitted from one end of an ideal cell to the other, as shown schematically in Fig. 2. In fact, Eq. (8) has been written to suggest that $\mu^r(n_l)$ and $\mu^l(n_r)$ are the input waves, and $\mu^l(n_l)$ and $\mu^r(n_r)$ are output waves, as viewed by the structural unit that is characterized by $[S]$.

Similar transformation of the state vectors in Eq. (3b) to wave vectors results in

$$\begin{Bmatrix} \mu^r(n+1_l) \\ \mu^l(n+1_l) \end{Bmatrix} = [Q(n)] \begin{Bmatrix} \mu^r(n_r) \\ \mu^l(n_r) \end{Bmatrix} \tag{10}$$

where

$$[Q(n)] = [D]^{-1}[P(n)][D] = [D]^{-1}[T(n)][D] \begin{bmatrix} \Lambda^{-1} & \\ & \Lambda \end{bmatrix} \tag{11}$$

Equation (10) can be recast in the form of Eq. (8), namely,

$$\begin{Bmatrix} \mu^l(n_r) \\ \mu^r(n+1_l) \end{Bmatrix} = [S(n)] \begin{Bmatrix} \mu^r(n_r) \\ \mu^l(n+1_l) \end{Bmatrix} \tag{12}$$

The elements in $[S(n)]$ can be obtained from those of $[Q(n)]$ as follows:

$$s_{11} = -q_{22}^{-1} q_{21} \tag{13a}$$

$$s_{12} = q_{22}^{-1} \tag{13b}$$

$$s_{21} = q_{11} - q_{12} q_{22}^{-1} q_{21} \tag{13c}$$

$$s_{22} = q_{12} q_{22}^{-1} \tag{13d}$$

In Eqs. (13a–13d) s_{ij} and q_{ij} are $p \times p$ submatrices of $[S(n)]$ and $[Q(n)]$, respectively, and the argument (n) is omitted in denoting the submatrices for simplicity.

It is physically meaningful to rename the submatrices of $[S(n)]$ as $r^r(n) = s_{11}$, $t^l(n) = s_{12}$, $t^r(n) = s_{21}$, and $r^l(n) = s_{22}$ and rewrite Eq. (12) as

$$\begin{Bmatrix} \mu^l(n_r) \\ \mu^r(n+1_l) \end{Bmatrix} = \begin{bmatrix} r^r(n) & t^l(n) \\ t^r(n) & r^l(n) \end{bmatrix} \begin{Bmatrix} \mu^r(n_r) \\ \mu^l(n+1_l) \end{Bmatrix} \tag{14}$$

The submatrices t and r are called the transmission and reflection matrices, respectively. The superscript for each of these submatrices signifies the direction of an incoming wave group to be transmitted or reflected. For example, $t^r(n)$ is a transmission matrix for an incoming wave group traveling in the right direction.

The matrix $[S(n)]$, which contains the transmission and reflection submatrices, is known as a scattering matrix. This particular scattering matrix characterizes the effects of disorder in the cell n that are lumped at the right end of cell n, as shown schematically in Fig. 2. In wave mechanics the concept of a scattering matrix is quite general; it characterizes the behavior of any identifiable structural element. In fact, the matrix $[S]$ in Eq. (8) is also a scattering matrix, in which the transmission and reflection matrices are $t^r = t^l = \Lambda$ and $r^r = r^l = 0$. These submatrices of $[S]$ are also related to those of a matrix $[Q]$ according to Eqs. (13a–13d), although, in this special case,

$$[Q] = \begin{bmatrix} \Lambda & 0 \\ 0 & \Lambda^{-1} \end{bmatrix} \tag{15}$$

It is interesting to remark that all scattering matrices are symmetric, a consequence of the reciprocity theorem for linear acoustic systems.

For a chain of cell units $1-N$ we may write

$$\begin{Bmatrix} \mu^r(N+1_l) \\ \mu^l(N+1_l) \end{Bmatrix} = [Q(N,1)] \begin{Bmatrix} \mu^r(1_l) \\ \mu^l(1_l) \end{Bmatrix} \tag{16}$$

where

$$[Q(N,1)] = [Q(N)][Q][Q(N-1)][Q]...[Q(1)][Q] \tag{17}$$

and where $[Q(n)]$ and $[Q]$ are given in Eqs. (11) and (15), respectively. Equation (16) can be recast in the form

$$\begin{Bmatrix} \mu^l(1_l) \\ \mu^r(N+1_l) \end{Bmatrix} = [S(N,1)] \begin{Bmatrix} \mu^r(1_l) \\ \mu^l(N+1_l) \end{Bmatrix} \tag{18}$$

in which

$$[S(N,1)] = \begin{bmatrix} r^r(N,1) & t^l(N,1) \\ t^r(N,1) & r^l(N,1) \end{bmatrix} \tag{19}$$

Elements of the matrix $[S(N,1)]$ are related to those of matrix $[Q(N,1)]$ according to Eqs. (13a–13d). From the second row of Eq. (18) we obtain

$$\mu^r(N+1_l) = t^r(N,1)\mu^r(1_l) + r^l(N,1)\mu^l(N+1_l) \tag{20}$$

Case of Monocoupling

We shall now consider the case of monocoupling in more detail. In this case the wave transfer matrices Q and the scattering matrices S become 2×2, and the transmission and reflection matrices reduce to the transmission and reflection coefficients. Moreover, we shall assume for the time being that cells $N+1$, $N+2$,..., ∞ are without disorder; thus, $\mu^l(N+1_l) = 0$. Then Eq. (20) is simplified to

$$\mu^r(N+1_l) = t^r(N,1)\mu^r(1_l) \tag{21}$$

The localization factor is defined as

$$\gamma = -\lim_{N\to\infty} \frac{1}{N} \ell n \left| \frac{\mu^r(N+1_l)}{\mu^r(1_l)} \right| \tag{22}$$

$$\mu^l(N+1_l) = 0$$

Upon using Eq. (21),

$$\gamma = -\lim_{N\to\infty} \frac{1}{N} \ell n |t^r(N,1)| \tag{23}$$

It implies that, if the limit in Eq. (23) exists, the transmitted wave has an average exponential decaying rate of γ per cell unit. This simple result can also be derived from an application of Furstenburg's theorem on products of random matrices.[17]

In passing, we remark that for the monocoupling case $t^r(N,1) = t^l(N,1)$, as can be proved from Eqs. (13a–13d) and from the fact that $|Q(N,1)| = 1$ since $[Q(N,1)]$ is a transfer matrix.[3]

Several specific cases will now be considered in the order of increasing complexity:

1) Small reflections: If all of the reflection coefficients due to disorder are small, so that the effect of multiple reflections is negligible, then $t^r(N,1)$ can be approximated by

$$t^r(N,1) = t^r(1)t^r(2)...t^r(N)\lambda^N \tag{24}$$

From Eq. (13b), $t^r(n) = t^l(n) = t(n) = q_{22}^{-1}(n)$. Whence

$$\gamma = -\ell n|\lambda| + \lim_{N\to\infty} \frac{1}{N} \sum_{n=1}^{N} \ell n|q_{22}(n)| \tag{25}$$

For disordered cells each uncertain parameter may be represented as a mean (or nominal value) plus a random variable. Then $q_{22}(n)$ are functions of such random variables that may be denoted by

$$q_{22}(n) = q_{22}[\boldsymbol{X}(n)] \tag{26}$$

where $\boldsymbol{X}(n) = \{X_1(n), X_2(n), ..., X_k(n)\}$ is a vector of random variables with zero means. It is reasonable to assume that $X_j(n)$ for different n are independent and identically distributed and that they form an ergodic sequence. Then the sequential averages in Eq. (25) may be replaced by ensemble averages; namely,

$$\gamma = -\ell n|\lambda| + \int \ell n|q_{22}(x)|p(x)\,dx \tag{27}$$

where $p(x)$ is the probability density of $\boldsymbol{X}(n)$, and the integrations are carried out in the domain of the random vector $\boldsymbol{X}(n)$. Equations (25) and (27) are equivalent with probability one. If $\boldsymbol{X}(n)$ is a k vector, the integral in Eq. (27) is actually a k-fold integral. Given the forms of $q_{22}[\boldsymbol{X}(n)]$ and the probability distribution of $\boldsymbol{X}(n)$, the integral can be evaluated at least numerically. In simple cases it can often be carried out in closed form, as shown later in an example.

If the system disorder is also small, then Eq. (27) may be approximated by

$$\gamma = -\ell n|\lambda| + \frac{\sigma_i^2}{2}\left\{\frac{\partial^2}{\partial x_i^2}\ell n|q_{22}(x)|\right\}_{x=0} \tag{28}$$

where σ_i^2 are the variances of $X_i(n)$. If, in addition, the structure is undamped and γ is evaluated at a wave-passage frequency, then $|\lambda| = 1$, and Eq. (28) reduces to

$$\gamma = \frac{\sigma_i^2}{2}\left\{\frac{\partial^2}{\partial X_i^2}\ell n|q_{22}(x)|\right\}_{x=0} \tag{29}$$

Equation (29) has been obtained previously by Kissel.[16]

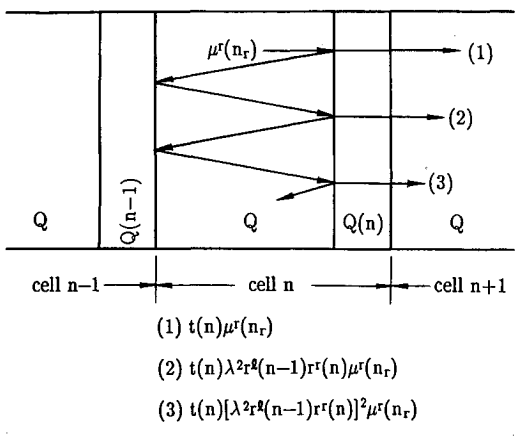

Fig. 3 Schematic representation of transmitted waves through the interface between cells n and $n+1$.

It should be emphasized that Eq. (27) is valid only for small reflection coefficients that imply that localization is weak. Equations (28) requires both small reflection coefficients and small disorder, and Eq. (29) additionally requires a zero damping and a wave-passage frequency.

2) Moderate reflections: If the reflection coefficients due to disorder are not sufficiently small, the approximation Eq. (24) may not be adequate. For improved accuracy certain multiple reflections will be considered. As shown in Fig. 3, the right-going wave $\mu^r(n_r)$ gives rise to a right-going transmitted wave $t(n)\mu^r(n_r)$ and a left-going reflected wave $r(n)\mu^r(n_r)$. The reflected wave travels through cell n and is itself partially reflected back at the interface between cells n and $n-1$. This backreflected wave also travels through cell n, whereupon it splits again into reflected and the transmitted parts. The latter is clearly $t(n)\lambda^2 r^l(n-1)r^r(n)\mu^r(n_r)$, and the former travels back through cell n, etc. Summing up all of the right-going waves that pass through the interface between cells n and $n+1$, we obtain

$$\begin{aligned}\mu^r(n+1_l) &= t(n)\{1 + \lambda^2 r^l(n-1)r^r(n) \\ &\quad + [\lambda^2 r^l(n-1)r^r(n)]^2 + \cdots\}\mu^r(n_r) \\ &= \frac{t(n)}{1-\lambda^2 r^l(n-1)r^r(n)}\mu^r(n_r)\end{aligned} \tag{30}$$

Thus,

$$t^r(N,1) = \prod_{n=1}^{N} \frac{t(n)\lambda}{1-\lambda^2 r^l(n-1)r^r(n)} \tag{31}$$

It follows from Eqs. (23) and (13a–13d) and the ergodicity assumption,

$$\begin{aligned}\gamma = &-\ell n|\lambda| + \int \ell n|q_{22}(x)|p(x)\,dx \\ &+ \iint \ell n\left|1 + \frac{\lambda^2 q_{12}(x_2)q_{21}(x_1)}{q_{22}(x_2)q_{22}(x_1)}\right| p(x_1)p(x_2)\,dx_1\,dx_2\end{aligned} \tag{32}$$

The third term is seen to provide added accuracy over Eq. (27). Equation (32) is valid for the case of moderate localization.

3) Strong reflection: Equation (32) may still be inadequate if the reflection coefficients are relatively large (although each cannot have a magnitude greater than one). However, higher accuracies can always be obtained by including more reflections at the interface between cells $n-1$ and $n-2$ is also taken into consideration, then

$$\mu^r(n+1_l) = t(n)\left[\frac{1}{1-a} + \frac{c}{(1-a)(1-b)(1-c)}\right]\mu^r(n_r) \tag{33}$$

where

$$a = \lambda^2 r^l(n-1)r^r(n) \tag{34a}$$

$$b = \lambda^2 r^l(n-2)r^r(n-1) \tag{34b}$$

$$c = t^2(n-1)\lambda^4 r^l(n-2)r^r(n) \tag{34c}$$

Again, using Eqs. (13a–13d) and invoking the ergodicity assumption,

$$\begin{aligned}\gamma = &-\ell n|\lambda| + \int \ell n|q_{22}(x)|p(x)\,dx - \iiint \ell n\left|\frac{1}{1+f_1(x_1,x_2)}\right. \\ &\left.\frac{f_2(x_1,x_2,x_3)}{[1+f_1(x_1,x_2)][(1+f_1(x_2,x_3)][1+f_2(x_1,x_2,x_3)]}\right| \\ &p(x_1)p(x_2)p(x_3)\,dx_1\,dx_2\,dx_3\end{aligned} \tag{35}$$

where

$$f_1(x_1,x_2)=\frac{\lambda^2 q_{12}(x_2)q_{21}(x_1)}{q_{22}(x_1)q_{22}(x_2)} \tag{36a}$$

$$f_2(x_1,x_2,x_3)=\frac{\lambda^4 q_{12}(x_3)q_{21}(x_1)}{q_{22}^2(x_2)q_{22}(x_3)q_{22}(x_1)} \tag{36b}$$

Formulas of still higher accuracies can be derived in an analogous manner.

Example

For illustration, the theory given in the preceding section is applied to an Euler-Bernoulli beam on evenly spaced hinge supports and with an additional torsional spring at each support, as shown in Fig. 4. In order to focus our attention on certain key issues in the theory without being obscured by unnecessary complexities, it is assumed that the beam is undamped and that only the torsional spring stiffnesses are random and are described by

$$k_n=k_0[1+X(n)], \qquad n=1,2,... \tag{37}$$

where k_0 is the average k_n and $X(n)$ are random variables with zero means. The other physical parameters are assumed to be deterministic, including the distances between neighboring supports l, the bending rigidity of the beam EI, and the mass of the beam per unit length m. Of course, the theory is applicable when several or all the parameters are random.

Several choices can be made for a typical cell unit in the analysis. The one selected for the following discussion is a typical beam element between two neighboring supports plus the entire right spring. The entire left spring is treated as belonging to the preceding cell. Then the transfer matrix for the nth cell is given by[3]

$$[T(n)]=\begin{bmatrix} \beta & \dfrac{\alpha}{\nu} \\ -\dfrac{\nu(1-\beta^2)}{\alpha}+\dfrac{\beta}{\delta}[1+X(n)] & \beta+\dfrac{\alpha}{\delta\nu}[1+X(n)] \end{bmatrix} \tag{38}$$

where

$$\delta=\frac{EI}{lk_0}, \qquad \nu=l\left(\frac{\omega^2 m}{EI}\right)^{1/4} \tag{39a}$$

$$\alpha=\frac{\cosh\nu\cos\nu-1}{\sinh\nu-\sin\nu} \tag{39b}$$

$$\beta=\frac{\sinh\nu\cos\nu-\cosh\nu\sin\nu}{\sinh\nu-\sin\nu} \tag{39c}$$

and ω = frequency.

The nondimensional δ is called the internal (cell-to-cell) coupling parameter, which is a measure of relative resistance against a rotation at a support between the beam element and an average torsional spring. If k_0 is very large so that δ is very small, then there is little cell-to-cell coupling, and strong localization is expected to occur.[15]

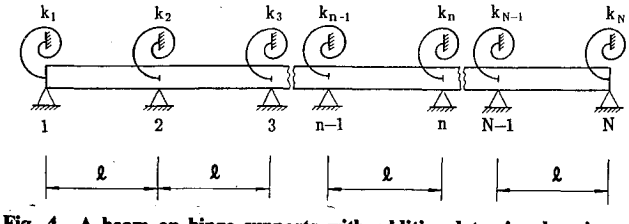

Fig. 4 A beam on hinge supports with additional torsional spring at each support.

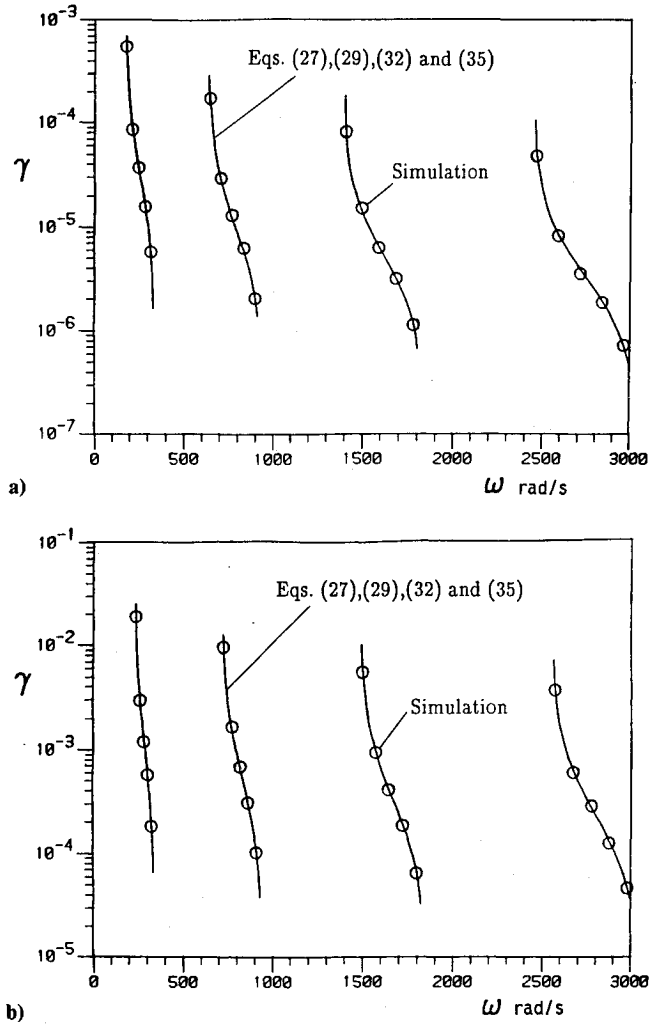

Fig. 5 Localization factors at frequencies in wave-passage frequency bands 1–4: a) $\delta=1$, $\sigma=0.1$; b) $\delta=0.1$, $\sigma=0.1$.

The transfer matrix $[T]$ for the ideal cell unit without disorder and the point transfer matrix $[P(n)]$ lumping the effect of disorder are obtained as follows:

$$[T]=\begin{bmatrix} \beta & \dfrac{\alpha}{\nu} \\ -\dfrac{\nu(1-\beta^2)}{\alpha}+\dfrac{\beta}{\delta} & \beta+\dfrac{\alpha}{\delta\nu} \end{bmatrix} \tag{40a}$$

$$[P(n)]=\begin{bmatrix} 1 & 0 \\ \dfrac{X(n)}{\delta} & 1 \end{bmatrix} \tag{40b}$$

The eigenvalues of transfer matrix $[T]$ are a reciprocal pair that may be denoted conveniently by $e^{\pm i\theta}$. It can be shown that θ can be found from[3]

$$\cos\theta=\beta+\frac{\alpha}{2\delta\nu} \tag{41}$$

and the wave-passage frequency bands are determined by the inequality

$$-1\le\beta+\frac{\alpha}{2\delta\nu}\le 1 \tag{42}$$

The wave-transfer matrix $[Q(n)]$ is obtained from

$$[Q(n)]=\begin{bmatrix} 1-iAX(n) & -iAX(n) \\ iAX(n) & 1+iAX(n) \end{bmatrix} \tag{43}$$

where $A=\alpha/(2\delta\nu\sin\theta)$.

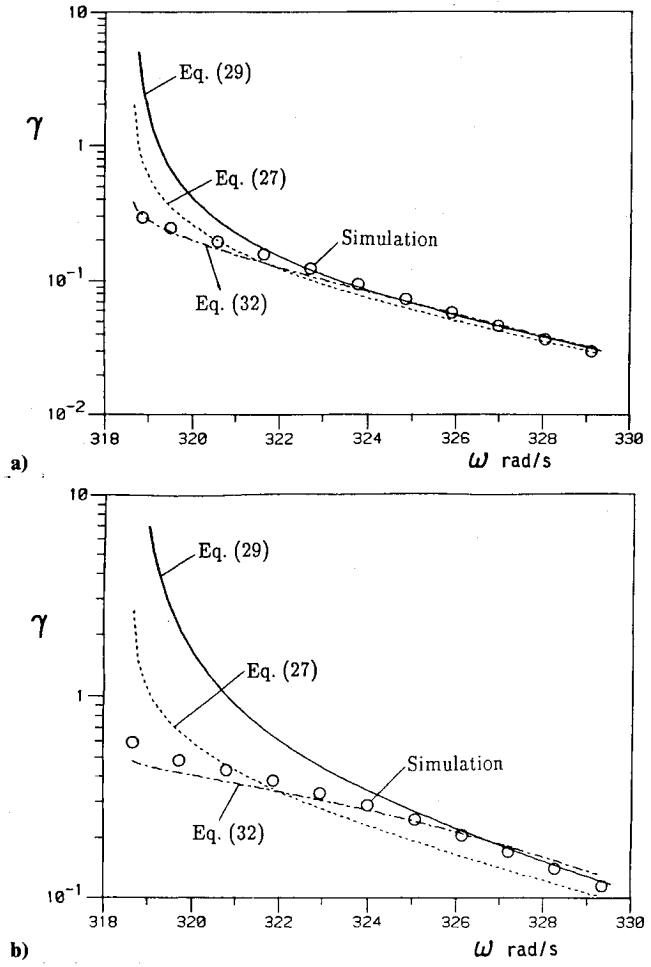

Fig. 6 Localization factors at frequencies in the lower half of the first wave-passage frequency band: a) $\delta = 0.01$, $\sigma = 0.25$; b) $\delta = 0.01$, $\sigma = 0.5$.

The following physical properties have been used in the numerical calculations: $l = 0.1651$ m, $m = 1.8043$ kg/m, and $EI = 0.3143$ N-m^2. In addition, $X(n)$ are assumed to be identically and uniformly distributed between $-\sqrt{3}\sigma$ and $\sqrt{3}\sigma$ where σ is the standard deviation of $X(n)$.

Substituting Eq. (43) into Eq. (27), we obtain an approximate localization factor for the case of wave-passage frequency and weak localization:

$$\gamma = \frac{1}{2}\ell n(1 + 3A^2\sigma^2) - 1 + \frac{1}{\sqrt{3}A\sigma}\tan^{-1}(\sqrt{3}A\sigma) \qquad (44)$$

where σ^2 is the variance of $X(n)$, which is assumed to be the same for all n. If, in addition, the disorder is small, we obtain from Eq. (29)

$$\gamma = \frac{\alpha^2\sigma^2}{8\delta^2\nu\sin^2\theta} \qquad (45)$$

For other cases for which the use of Eq. (27), (32), or (35) is more appropriate, numerical integrations are generally required using an assumed probability density for $X(n)$.

The computed localization factors in the first four wave-passage frequency bands are shown in Figs. 5a and 5b for $\delta = 1$, $\sigma = 0.1$ and for $\delta = 0.1$, $\sigma = 0.1$, respectively. Except for frequencies very close to the lower boundary of a wave-passage frequency band (not shown in Fig. 5), all four equations, Eqs. (27), (29), (32), and (35), yield essentially the same results and are in excellent agreement with those obtained from Monte Carlo simulations, also shown in the figure. That the values of the localization factors are below 0.02 is an indication of weak localization in these cases. At the lower boundary of a wave-passage frequency band, the deformations of two neighboring spans tend to be out of phase (exactly out of phase for an ideal periodic structure) and the torsional springs at the supports influence the beam motion to a great extent. Therefore, even a small disorder of the torsional springs may give rise to strong localization. On the other hand, the deformations of two neighboring spans are nearly in phase at the upper boundary of a wave-passage frequency, and the torsional springs have little effect on the beam motion. Hence, their disorder is relatively unimportant.

The Monte Carlo simulations referred to earlier were carried out by multiplying a large number of random wave-transfer matrices at a given frequency to obtain one realization of

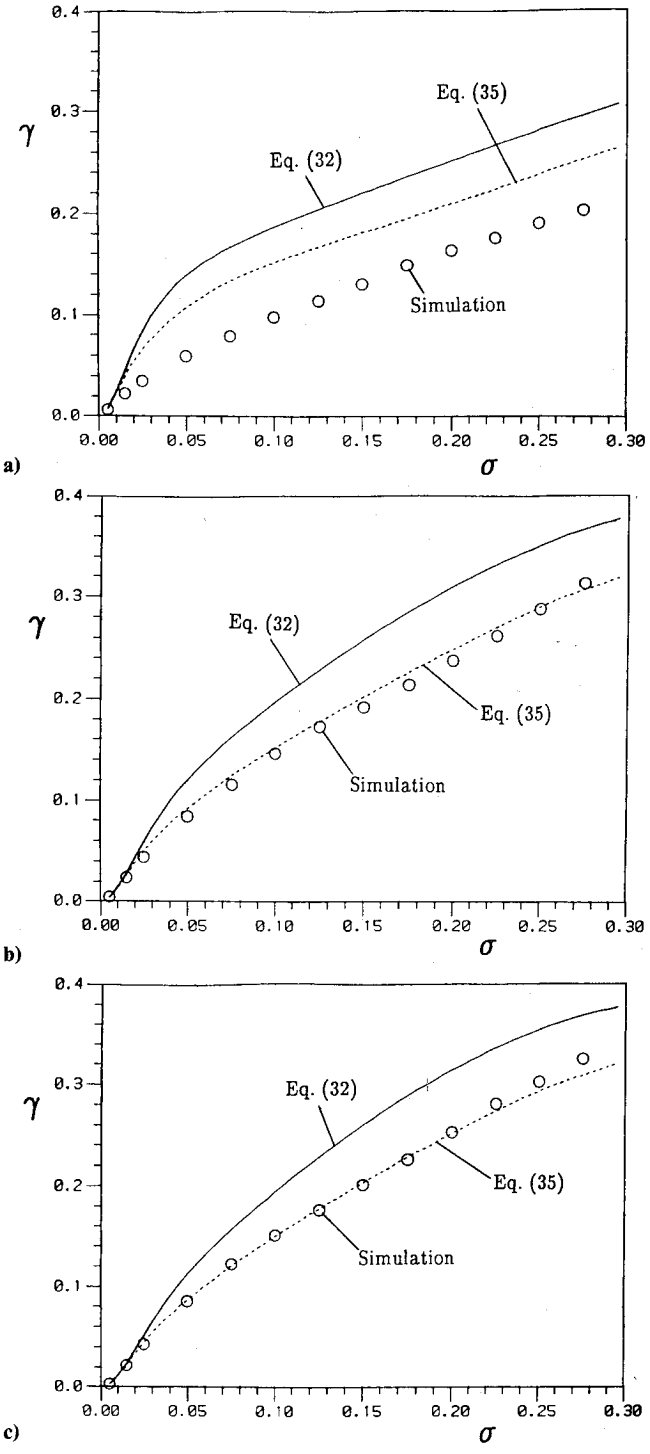

Fig. 7 Localization factors at frequencies near the lower boundaries of the first wave-passage frequency band: a) $\delta = 0.1$, $\omega = 232.5$ rad/s; b) $\delta = 0.01$, $\omega = 318.7$ rad/s; c) $\delta = 0.001$, $\omega = 339.72$ rad/s.

the wave-transfer matrix for the overall N-span system according to Eq. (17) and thus one realization of $t^r(N,1)$. The values of $N^{-1}\ell_n|t^r(N,1)|$ for different realizations were averaged over a sufficient number of realizations to obtain an estimate for the localization factor. This procedure is different from the one adopted by Kissel,[16] in which an average is taken of a large number of $\ell_n|t(n)|$, where each $t(n)$ is the transmission coefficient of one realization of a single cell. It is felt that our simulation procedure is physically more meaningful. In our simulations, 300 cells were used in each realization, and the average was taken over 2000 realizations.

Figures 6a and 6b depict the computed localization factors for systems with $\delta = 0.01$, $\sigma = 0.25$ and $\delta = 0.01$, $\sigma = 0.50$, respectively, and with frequencies falling within the lower part of the first wave-passage frequency band. It is seen that the closer a frequency is to the lower boundary of the wave-passage frequency band, the more Eqs. (27) and (29) overestimate the localization factor, because the reflection coefficients become larger and the effect of multiple reflection is no longer negligible. By taking the reflections in only one cell on the immediate left to account, Eq. (32) yields much more accurate results than those of Eqs. (27) and (29) when compared with simulation results. Figure 6 shows that, for a beam system with fixed δ and σ, localization is strong at a frequency very near to the lower boundary of a wave-passage frequency band, and it becomes weaker as the frequency increases. This implies that the disorder to internal coupling ratio (σ/δ) is not the only factor in determining the intensity of localization, as once suggested; the frequency location relative to a wave-passage band is at least another factor. Other factors might be also important in more complicated systems.

Results obtained from Eq. (27) are generally more accurate than those obtained from Eq. (29). However, exceptions can occur, as shown in the higher-frequency region in Figs 6a and 6b. This is due to the fact that both equations are approximate. Although Eq. (27) essentially retains more terms in the approximation, it does not follow that those additional terms will increase the accuracy consistently.

As pointed out earlier, localization may be strong at frequencies near the lower boundaries of wave-passage frequency bands, even when the disorder is relatively small. Three such cases, 1) $\delta = 0.1$, $\omega = 232.5$ rad/s; 2) $\delta = 0.01$, $\omega = 318.7$ rad/s; and 3) $\delta = 0.001$, $\omega = 339.72$ rad/s, have been examined in more detail. The results obtained are shown in Figs. 7a–7c, respectively, with varying standard deviation of disorder σ. In all of these cases Eq. (32) is clearly inadequate. Equation (35) leads to satisfactory results for cases 2 and 3. For case 1, in which the disorder is also greater, Eq. (35) is still inadequate, although it is much superior to Eq. (32). The use of even higher-order approximations is suggested.

Concluding Remarks

The successive improvement in accuracy and the inclusion of structural damping are two important features in the proposed perturbation scheme for the computation of localization factors for disordered periodic structures. The first feature permits a unified approach to any disorder to internal coupling ratio and at any frequency location relative to the lower boundaries of the wave-passage frequency band. They are shown to be the governing factors for the degree of localization in the illustrative examples. The second feature permits the consideration of practical structures. The formulation based on a generic disordered periodic structure is also an advantage, since it is not restricted to a specific type of system, and it facilitates future extension to the case of multiple coupling between neighboring cells.

Acknowledgments

This paper is prepared under Grant AFOSR-88-0005 from the Air Force Office of Scientific Research, Air Force Systems Command, USAD, monitored by George Haritos. The U.S. Government is authorized to reproduce and distribute reprints for governmental purposes, notwithstanding any copyright notation thereon. Most helpful discussions with S. T. Ariaratnam, Y. Yong, and R. C. Zhang, and suggestions from the reviewers are gratefully acknowledged.

References

[1]Miles, J. W., "Vibration of Beams on Many Supports," *Journal, Engineering Mechanics Division, ASCE*, Vol. 82, No. EM1, Jan. 1956, pp. 1–9.

[2]Lin, Y. K., "Free Vibration of Continuous Beams on Elastic Supports," *Journal of Mechanical Science*, Vol. 4, Sept.–Oct. 1962, pp. 409–423.

[3]Lin, Y. K., and McDaniel, T. J., "Dynamics of Beam-Type Periodic Structures," *Journal of Engineering for Industry*, Vol. 91, Nov. 1969, pp. 1133–1141.

[4]Mead, D. J., "Free Wave Propagation in Periodically-Supported Infinite Beam," *Journal of Sound and Vibration*, Vol. 11, No. 2, 1970, pp. 181–197.

[5]Mead, D. J., "Wave Propagation and Natural Modes in Periodic Systems: I. Mono-Coupled Systems, II. Multi-Coupled Systems, With and Without Damping," *Journal of Sound and Vibration*, Vol. 40, No. 1, 1975, pp. 1–39.

[6]Yong, Y., and Lin, Y. K., "Propagation of Decaying Waves in Periodic and Piecewise Periodic Structures of Finite Length," *Journal of Sound and Vibration*, Vol. 129, No. 2, 1989, pp. 99–118.

[7]Soong, T. T., and Bogdanoff, J. L., "On the Natural Frequencies of a Disordered Linear Chain of N Degrees of Freedom," *Int. Journal of Mechanical Sciences*, Vol. 5, 1963, pp. 237–265.

[8]Soong, T. T., and Bogdanoff, J. L., "On the Impulsive Admittance and Frequency Response of a Disordered Linear Chain of N-Degrees of Freedom," *Int. Journal of Mechanical Sciences*, Vol. 6, 1964, pp. 225–237.

[9]Lin, Y. K., and Yang, J. N., "Free Vibration of a Disordered Periodic Beam," *Journal of Applied Mechanics*, Vol. 41, No. 2, 1974, pp. 383–391.

[10]Yang, J. N., and Lin, Y. K., "Frequency Response Functions of a Disordered Periodic Beam," *Journal of Sound and Vibration*, Vol. 38, No. 3, 1975, pp. 317–340.

[11]Anderson, P. W., "Absence of Diffusion in Certain Random Lattices," *Physical Review*, Vol. 109, No. 5, 1958, pp. 1492–1505.

[12]Lee, P., "Disordered Solids," *Physics Today*, Vol. 41, Dec. 1988, pp. 22–23.

[13]Hodges, C. H., "Confinement of Vibration by Structural Irregularity," *Journal of Sound and Vibration*, Vol. 82, No. 3, 1982, pp. 441–444.

[14]Hodges, C. H., and Woodhouse, J., "Vibration Isolation from Irregularity in a Nearly Periodic Structure: Theory and Measurements," *Journal of Acoustic Society of America*, Vol. 74, No. 3, 1983, pp. 894–905.

[15]Pierre, C., "Weak and Strong Vibration Localization in Disordered Structures: A Statistical Investigation," *Journal of Sound and Vibration*, Vol. 139, No. 1, 1990, pp. 111–132.

[16]Kissel, G. J., "Localization in Disordered Periodic Structures," PhD Dissertation, Massachusetts Institute of Technology, Cambridge, MA, 1988.

[17]Furstenberg, H., "Noncommuting Random Products," *Transactions of the American Mathematical Society*, Vol. 108, No. 3, 1963, pp. 377–428.

[18]Oseledets, V. I., "A Multiplicative Ergodic Theorem," *Transactions of the Moscow Mathematical Society*, Vol. 19, 1968, pp. 197–231.

[19]Pestel, E. C., and Leckie, F. A., *Matrix Methods in Elastomechanics*, McGraw-Hill, New York, 1963.